Substrate-Controlled Group-Selective Radical Cyclizations. A New Strategy for Stereocontrolled Transformations of Diastereomeric Reactive Intermediates

Dennis P. Curran,* Hongyan Qi, Nicholas C. DeMello, and Chien-Hsing Lin

Department of Chemistry, University of Pittsburgh Pittsburgh, Pennsylvania, 15260

Received June 1, 1994

The creation of stereogenic sp^3-hybridized carbon atoms[1] occurs through one of two fundamental processes: diastereoface selection (face selectivity) or diastereotopic group selection (group selectivity). A large number of face-selective radical reactions are now known,[2] and we have recently reported several group-selective radical cyclizations that are under chiral auxiliary control.[3] We now communicate an example of a highly group-selective radical cyclization under substrate control.[4] This reaction serves as a model for a more unique cyclization in which modest group selectivity is observed even though there is no diastereotopic group-selective step in the transformation. Our observations and analysis suggest a new strategy for stereocontrol in reactions of diastereomeric reactive intermediates.

The preparation and cyclization of the model substrate **1** are shown in eq 1. Reductive alkylation of methyl benzoate with

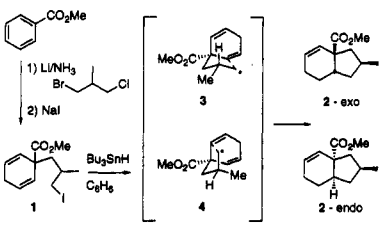

(1)

racemic 1-bromo-3-chloro-2-methylpropane followed by Finkelstein reaction provided cyclohexadiene **1** in 76% yield. Cyclization of **1** with 1.2 equiv of Bu_3SnH under standard conditions (0.02 M, 5% AIBN) at 80 °C provided an inseparable mixture of **2-*exo*** and **2-*endo*** in a ratio of 94/6 in 82% yield. Cyclization at −78 °C (Et_3B initiation)[5] gave an improved ratio of 97/3 (66% yield).[6] The group selectivity for this reaction is consistent with Beckwith's guidelines for stereoselectivity in radical cyclizations.[7] Chairlike transition state **3** with the "equatorial" methyl group leads to **2-*exo***. This is favored over chairlike transition state **4** (leading to **2-*endo***) because addition of the radical to the diastereotopic alkene places the methyl group in an "axial" orientation. Such substrate-controlled group-selective radical cyclizations have good potential for use in asymmetric synthesis.[8]

(1) Mislow, K.; Siegel, J. *J. Am. Chem. Soc.* **1984**, *106*, 3319.
(2) Reviews: (a) Porter, N. A.; Giese, B.; Curran, D. P. *Acc. Chem. Res.* **1991**, *24*, 296. (b) Smadja, W. *Synlett* **1994**, 1.
(3) (a) Curran, D. P.; Geib, S. J.; Lin, C.-H. *Tetrahedron: Asymmetry* **1994**, *5*, 199. (b) For an example of the reverse reaction (group-selective hydrogen abstraction to generate an sp^2 center from an sp^3 center), see: Sugimura, T.; Goto, S.; Koguro, K.; Futagawa, T.; Misaki, S.; Morimoto, Y.; Yasuoka, N.; Tai, A. *Tetrahedron Lett.* **1993**, *34*, 505.
(4) We are aware of one example of a substrate-controlled group selectivity, though the level of selectivity is very low. See compound **17** in: Beckwith, A. L. J.; Roberts, D. H. *J. Am. Chem. Soc.* **1986**, *108*, 5893.
(5) Mirura, K.; Ichinose, Y.; Nozaki, K. J.; Fugami, K.; Oshima, K.; Utimoto, K. *Bull. Chem. Soc. Jpn.* **1989**, *62*, 143.
(6) Hydrolysis of the **2-*exo*/2-*endo*** mixture (NaOH/MeOH) and treatment with NH_3 provided a crystalline ammonium salt derived from **2-*exo***, whose structure was solved by X-ray crystallography. See supplementary material for details.
(7) (a) Beckwith, A. L. J.; Schiesser, C. H. *Tetrahedron* **1985**, *41*, 3925. (b) Spellmeyer, D. C.; Houk, K. N. *J. Org. Chem.* **1987**, *52*, 959.
(8) Optically pure **1** is readily prepared from commercially available (*R*)-3-bromo-2-methylpropanol: Qi, H. unpublished results.

Table 1. Reduction of **6** at Varying Ph_3SnH Concentrations[a]

entry	$[Ph_3SnH]$	$Ph_3SnH/6$	7-*exo*[b]	7-*endo*[b]	8[b]
1	0.02	2.1	50	50	0
2	0.10	15.5	54.1	45.5	0.4
3	0.24	12.1	56.6	41.1	2.3
4	0.50	12.9	59.6	28.8	11.6
5	0.74	10.2	60.2	26.0	13.8
6	1.01	13.6	57.5	20.2	22.3
7	1.49	11.3	54.3	19.7	27.0
8	2.01	15.2	52.1	15.1	32.8

[a] Reactions were conducted in C_6D_6 at 75 °C in the presence of 5% AIBN (initiator) and 0.13–0.20 equiv of 1,4-dimethylbenzene (NMR integration standard). [b] Yields were determined by integration of methyl resonances in the ^1H NMR spectrum against the internal standard. Total observed yields varied from 97% to 103%. The reported yields are corrected to 100%.

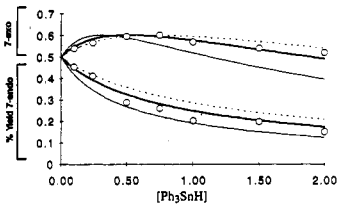

Figure 1. Yields of **7-*exo*** and **7-*endo*** at varying $[Ph_3SnH]$. The lines represent values calculated from the kinetic model using (from inside to out) k_{fast} values of 3×10^7, 5×10^7, and 7×10^7 s^{-1} with a k_{fast}/k_{slow} ratio of 4.0 and a k_H of 2.0×10^7 s^{-1}.

The preparation and cyclization of substrate **6** are shown in eq 2. Deprotonation of **5** and alkylation with tris(iodomethyl)-

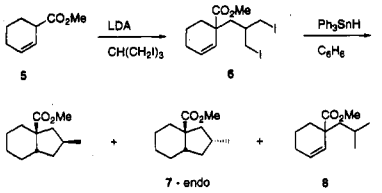

(2)

methane provided racemic **6** in 65% yield. In contrast to substrate **1**, where two diastereotopic alkenes competed for a single radical, substrate **6** presents two diastereotopic radical precursors competing for a single alkene. The data for the cyclization of **6** at varying concentrations of Ph_3SnH are summarized in Table 1. A total of three products, **7-*exo***, **7-*endo***, and **8**, were observed. The structure of **8** was established by synthesis of an authentic sample (by alkylation of the enolate of **5** with *i*-BuI). Catalytic hydrogenation of a 15/1 mixture of **2-*exo*/2-*endo*** provided a 15/1 mixture of **7-*exo*/7-*endo***, thus establishing the configurations of these products. Reduction of **6** at 0.02 M provided **7-*exo*** and **7-*endo*** in a ratio of 50/50 (Table 1, entry 1). This experiment suggests that no group selectivity can be observed with **6**. However, selectivity is observed as the Ph_3SnH concentration increases (Table 1, entries 2–8), and the data show several clear trends: (1) the yield of **7-*exo*** climbs from 50% to 60% (entries 2–5) before beginning a slow desent; (2) the ratio of **7-*exo*/7-*endo*** continuously climbs from its initial level of 50/50; and (3) the yield of the doubly reduced product **8** steadily increases.

The mechanistic framework for interpreting these observations is shown in Scheme 1. Since the iodomethyl groups in **6** are diastereotopic, a cursory analysis suggests that group selectivity will be established at the stage of iodine abstraction by $Ph_3Sn^{\cdot}$. The results in Table 1, entry 1, show that this is indeed the case at low tin hydride concentrations. The rate of abstraction of either diastereotopic iodine atom from **6** by $Ph_3Sn^{\cdot}$ is probably close to diffusion controlled[9] and occurs with equal probability

(9) Ingold, K. U.; Lusztyk, J.; Scaiano, J. C. *J. Am. Chem. Soc.* **1984**, *106*, 343.

0002-7863/94/1516-8430$04.50/0

Scheme 1

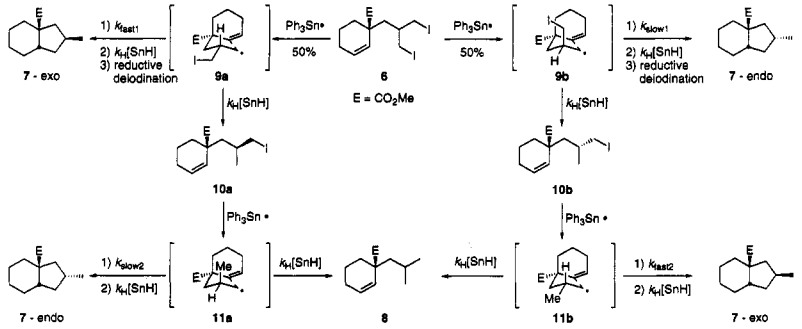

to provide diastereotopic radicals **9a** and **9b**. At low tin hydride concentrations, cyclizations of both **9a** and **9b** are much faster than bimolecular hydrogen transfer. Cyclization of **9a**, followed by hydrogen transfer from Ph_3SnH and reductive deiodination of the remaining iodide provides **7-*exo***. A similar sequence of cyclization, hydrogen transfer, and reductive deiodination provides **7-*endo*** from **9b**.

As the tin hydride concentration increases, the ratio **7-*exo*/7-*endo*** no longer reflects the rate ratio in the initial iodine abstraction from **6**. At a critical tin hydride concentration, the reductions of radicals **9a,b** begin to compete with cyclizations. These radicals cyclize at different rates: radical **9a** resembles model radical **3a** (eq 1), so it should cyclize more rapidly than radical **9b**, which resembles model **4a**. Because radical **9b** cyclizes more slowly than **9a**, it will be trapped preferentially by tin hydride to provide **10b**. Abstraction of the remaining iodide from **10b** produces radical **11b**, which now partitions between direct reduction to give **8** and cyclization (followed by hydrogen transfer) to give **7-*exo***. Since radical **11b** now resembles the faster cyclizing radical **3**, its partitioning between cyclization and hydrogen transfer (k_{fast2}/k_H[SnH]) is higher than that of its precursor **9b** (k_{slow1}/k_H[SnH]). In short, at low concentrations of tin hydride, radical **9b** leads only to **7-*endo***, and **9a** leads only to **7-*exo***, but as the tin hydride concentration increases, intermediates **9a,b** are subject to kinetic resolution by competition with hydrogen abstraction. Furthermore, each of the two resulting monoreduced side products **10a,b** is subject to a second kinetic resolution, enhancing the yield and diasteriomeric excess of the two cyclized products (**7-*exo*/7-*endo***) of the first resolution. With further increase of the tin hydride concentration, the rate of hydrogen transfer becomes competitive with the faster cyclization, and the yield of **7-*exo*** declines; however, the ratio of **7-*exo*/7-*endo*** continues to increase.

The mechanism in Scheme 1 contains 20 different steps, all of which are irreversible. Despite this complexity, the scheme was analyzed with only three key assumptions: (1) that the partitioning of **6** to **9a/9b** always occurs with 50/50 ratio; (2) that $k_{fast1} = k_{fast2}$; and (3) that $k_{slow1} = k_{slow2}$. The first postulate is supported by the results of the low tin hydride concentration experiment (entry 1). The other two postulates are intuitively reasonable (radicals **9a/11b** and **9b/11a** differ only in having CH_2I or CH_3 substituent on the cyclizing radical) and have experimental support.[10] We derived equations describing the product ratios of **7-*exo***, **7-*endo***, and **8** as a function of k_{fast} and k_{slow}. By varying k_{fast} and k_{slow}, we fit the function to the data and arrived at a value of 5×10^7 s^{-1} for k_{fast} (at 80 °C) and a value of 4 for the ratio of k_{fast}/k_{slow}. Figure 1 illustrates the sensitivity of the function to slight variations in k_{fast}. The rate constant ratio (4) is lower than the ratio (about 15) that we expected from the model (eq 1).

Though it is not highly selective, the overall transformation of **6** to **7-*exo*/7-*endo*** at high tin hydride concentrations is clearly an example of a diastereotopic group-selective process. However, unlike most existing examples of group selectivity, there is no single step that occurs in which two diastereotopic groups are differentiated (diastereotopic iodides react in the first step, but without selectivity). The analysis of Scheme 1 embodies a general strategy for group-selective reactions of reactive intermediates that are converted to products at different rates. In this case, the diastereotopic reactive intermediates are radicals **9a** and **9b**, and they cyclize at different rates. Selectivity is imposed by setting the rate of a third reaction (in this case, hydrogen transfer from tin hydride) in a range that is competitive with the slower of the two reactions of the reactive intermediates. This then traps the slower reacting intermediate (**9b**), thereby decreasing the yield of one product (**7-*endo***) and at the same time opening a new pathway to increase the yield of its competitor (**7-*exo***).

This indirect process for stereocontrol is probably useful only for reactive intermediates because the maximum yield of products is always less than the rate constant ratio. In the example at hand, the maximum theoretical yield of **7-*exo*** is 60% at a k_{fast}/k_{slow} ratio of 4. In contrast, a traditional direct competition of diastereotopic groups with a rate constant ratio of 4 would give an 80% yield of the major product. The direct competition is superior because no trapping reagent is required to effect selectivity. In the indirect process, some reactive intermediates are always lost to reactions with the trap (in Scheme 1, **8** forms). Nonetheless, we expect that the process will be useful because it amplifies the selectivity of a reaction by increasing the yield of the major product. Most existing processes that amplify the selectivity of a group-selective (for example, the Sharpless epoxidation[11]) or face-selective (for example, the Jacobsen epoxidation[12]) reaction do so by decreasing the yield of the minor product. As the ratio k_{fast}/k_{slow} increases, so does the maximum possible yield of the major product. We calculate the following maximum yields of major products at k_{fast}/k_{slow} ratios of 10, 68%; 100, 89%; and 1000, 98%. Our current efforts are directing at designing and studying radical reactions with a range of rate constant ratios to see if this model can be validated.

Acknowledgment. We thank the National Science Foundation and the National Institutes of Health for funding this work. We are very grateful to Professors C. Walling and C. Wilcox for their help in deriving the rate equations and to Dr. S. Geib for solving the crystal structures.

Supplementary Material Available: Full experimental details for the experiments described in eqs 1 and 2, a derivation of the rate laws used in the kinetic analysis, and details of the crystal structure of the ammonium salt derived from **2-*exo*** (18 pages). This material is contained in many libraries on microfiche, immediately follows this article in the microfilm version of the journal, and can be ordered from the ACS; see any current masthead page for ordering information.

(10) (a) The dibromide analog of **6** has also been reduced and gives results similar to those of the diiodide. (b) Iodides **10a/b** have been prepared and cyclized. The observed product ratios replicate the predictions from the model.

(11) Schreiber, S. L.; Schreiber, T. S.; Smith, D. B. *J. Am. Chem. Soc.* **1987**, *109*, 1525.

(12) Zhang, W.; Lee, N. H.; Jacobsen, E. N. *J. Am. Chem. Soc.* **1994**, *116*, 425.